DENTAL MATERIALS XXX (2015) XXX–XXX

Available online at www.sciencedirect.com

ScienceDirect

journal homepage: www.intl.elsevierhealth.com/journals/dema

Tuning photo-catalytic activities of TiO_2 nanoparticles using dimethacrylate resins☆

Jirun Sun[a,*], *Stephanie S. Watson*[b], *David A. Allsopp*[a], *Debbie Stanley*[b], *Drago Skrtic*[a]

[a] *Dr Anthony Volpe Research Center, American Dental Association Foundation, Gaithersburg, MD 20899, USA*
[b] *Polymeric Materials Group, Materials and Structural Systems Division, National Institute of Standards and Technology, Gaithersburg, MD 20899, USA*

ARTICLE INFO

Article history:
Received 12 February 2015
Received in revised form
20 August 2015
Accepted 30 November 2015
Available online xxx

Keywords:
Titanium dioxide nanoparticles
Free radical
Photo-catalytic activities
Dental resins
Nano-composites
Dimethacrylates
Wettability

ABSTRACT

Objective. The unique photo-catalytic activities (PCAs) of titanium dioxide nanoparticles (TiO_2 NPs) made them attractive in many potential applications in medical devices. The objective of this study is to optimize the benefits of PCAs of TiO_2 NPs through varying chemical structures of dimethacrylate resins.

Methods. TiO_2 NPs were functionalized to improve the PCAs and bonding to the resins. The PCAs of TiO_2 NPs were evaluated using electron paramagnetic resonance (EPR) and UV–vis spectroscopy to determine the amount of the radicals generated and the energy required for their production, respectively. The beneficial effects of the radicals were assessed through: (1) the improvement of degree of vinyl conversion (DC) and (2) modification of resin hydrophilicity. One-way ANOVA with a 95% confidence interval was used to indicate the significant differences between the experimental groups.

Results. EPR and UV–vis results clearly showed that the functionalization of TiO_2 NPs enhanced PCAs in terms of generating radicals under visible light irradiation. The presence of hydroxyl and carboxylic acid functionalities played an important role in DC enhancement and hydrophilicity modification. The DC could be increased up to 22% by adding only 0.1 wt% TiO_2 NPs. Viscosity of the resins had minimal or no role in DC improvement through TiO_2 NPs. In resins with abundant hydroxyl groups, radicals were more effective in making the resin more hydrophilic.

Significance. Knowledge learned from this study will help formulating nano-composites with optimized use of TiO_2 PCAs as co-initiators for photo-polymerization, additives for making super-hydrophilic materials and/or antibacterial agents.

☆ Official contribution of the National Institute of Standards and Technology; not subject to copyright in the United States.

* *Corresponding author at*: 100 Bureau Drive, Stop 8546 Gaithersburg, MD 20899-8546, USA. Tel.: +1 301 975 5439; fax: +1 301 963 9143.
E-mail address: jsun@nist.gov (J. Sun).

http://dx.doi.org/10.1016/j.dental.2015.11.021
0109-5641/

1. Introduction

The unique photo-catalytic activities (PCAs) of TiO_2 nanoparticles [1–4] make them attractive in many potential applications including self-cleaning surfaces [5,6], antibacterial medical devices [7] and high performance dental composites [8,9]. Besides their PCAs, TiO_2 NPs are inexpensive and chemically stable; they also have excellent mechanical properties (elastic modulus of TiO_2 is 230 GPa) [1]. Traditionally, TiO_2 is used as a pigment additive in materials, including cosmetic and constructive materials, because of its high refractive index (n); TiO_2 particles are also used in dental composites to match the color, translucence and opalescence of natural tooth for aesthetic purposes [10,11]; and its PCAs are attracting more and more attention because they are the basis of TiO_2 NPs utility in antimicrobial agents [3,7,12], initiators for photo-polymerization [9], solar cells [4], and super-hydrophilic surfaces for self-cleaning materials [13]. The PCAs indicate the capability of TiO_2 NPs to utilize energy from light irradiation and generate resources for the above applications without consuming themselves, which are typically evaluated by the NPs' capability to: (1) absorb light, especially visible light; and (2) produce and preserve radicals (in the form of electrons and holes) [2]. The processes of PCAs from light irradiation to final applications are: TiO_2 NPs (<50 nm) utilize energy from light irradiation to generate electrons and holes; through them, water and oxygen are converted into powerful free radicals and oxidation agents: superoxide and hydroxyl radical [1,14,15], which are valuable in the above applications and biological processes.

Free radicals are vital in biological processes. They are used for intracellular killing of bacteria in phagocytic cells, including granulocytes and macrophages; also they are implicated in redox signaling processes [16,17]. The two most important oxygen-centered radicals are superoxide and hydroxyl radical [17]. Both of them are strong oxidants, e.g., hydroxyl radicals are four times stronger than hydrogen peroxides. Due to their reactivity, excessive amount of free radicals may cause unwanted side effects resulting in damage of cells and biological bodies [18,19]. Because they are necessary for life, there are many biological defense mechanisms to minimize free-radical-induced damage and to repair damage that occurs, in which antioxidants, including vitamin A, vitamin C and vitamin E, play a key role; and some functional groups including hydroxyl groups, carboxyl groups, and amine groups are essential for their antioxidant purposes [20–22].

Successful implementation of the unique properties of TiO_2 NPs in resin can lead to significant enhancement of resin performance and provide flexibility in controlling the resin network structure and functionality, thus creating new materials capable of meeting the complex requirements for functionality and durability. Our previous studies demonstrated that: (1) TiO_2-containing resins yielded significantly stronger dental adhesives (the mean shear bond strength increased approximately 30% when 0.1 wt% of functionalized TiO_2 NPs were added) [9] than the pure resin counterparts; (2) The addition of functionalized TiO_2 NPs dramatically improved the performance of resins, including significantly enhanced degree of vinyl conversion (DC), elastic modulus (E), hardness (H) [9]. Learning from the key functional groups of antioxidants in biological defense systems, experiments were designed to understand how the chemical structure of resins influences the application of the free radicals generated by TiO_2 NPs. The PCAs of TiO_2 NPs were evaluated using electron paramagnetic resonance (EPR) and UV–vis spectroscopy to determine the amount of radicals generated and the energy required for their production, respectively. The beneficial effects of the free radicals were assessed through the improvement of degree of vinyl conversion (DC; quantified by Fourier Transform Infrared spectroscopy) and the modification of hydrophilicity of dimethacrylate resins [quantified by measuring the water contact angle (WCA)]. The viscosity and the number of hydroxyl and/or carboxyl groups of the experimental resins were then correlated with the PCAs of TiO_2 nanoparticles.

2. Materials and methods

2.1. Materials and sample preparation

Resin[1] monomers, ethoxylated-bisphenol-A-dimethacrylate (EBPDMA), 2-bis(4-(2-hydroxy-3-methacryloxypropoxy) phenyl)propane) (Bis-GMA), triethyleneglycol dimethacrylate (TEGDMA), pyromellitic-glycerol-dimethacrylate (PMGDM) and/or hydroxyethyl-methacrylate (HEMA), were gifts from Esstech Inc (Essington, PA, USA). Their chemical structures are shown in Fig. 1. The initiators, camphorquinone (CQ) and ethyl 4-N, N-dimethylaminobenzoate (4E) were purchased from Sigma–Aldrich (St. Louis, MO, USA). CQ (0.2 wt%) and 4E (0.8 wt%) were mixed with resin monomers (99 wt%) before adding nanoparticles. Methylene blue (MB) and acrylic acid was also obtained from Sigma–Aldrich. Titanium dioxide nanoparticles (P25, AEROXIDE TiO_2), a known photo-catalytically active material composed of both anatase and rutile phases, were provided by Evonik Industries (Essen, Germany). All reagents were used as received.

The P25 TiO_2 NPs were functionalized with acrylic acid following a modified method described previously [9,23]; the product was labeled as AP25. Briefly, acrylic acid (7.2 g), water (0.8 g), hexane (8 g) and P25 (0.2 g) were combined and sonicated at 0 °C for 30 min using a 130 W ultrasonic processor (model# GEX 130PB, Cole-Parmer, USA). The mixture was then agitated at 500 RPM at 37 °C for 48 h. A resulting milky mixture was transferred into a 50 mL centrifuge tube and centrifuged at 13,000 rpm for 60 min. The AP25 precipitate was collected and redistributed in 25 mL of ethanol, which was centrifuged again at 13,000 rpm for 60 min. The redistribution and centrifugation steps were repeated two more times to remove the excess acrylic acid loosely absorbed on the NPs. The same sonication setup was also used to prepare AP25 organosols by dispersing AP25 powder in ethanol at 0.1% by mass. These

[1] Certain equipment, instruments or materials are identified in this paper to adequately specify the experimental details. Such identification does not imply recommendation by the National Institute of Standards and Technology, nor does it imply the materials are necessary the best available for the purpose.

Please cite this article in press as: Sun J, et al. Tuning photo-catalytic activities of TiO_2 nanoparticles using dimethacrylate resins. Dent Mater (2015), http://dx.doi.org/10.1016/j.dental.2015.11.021

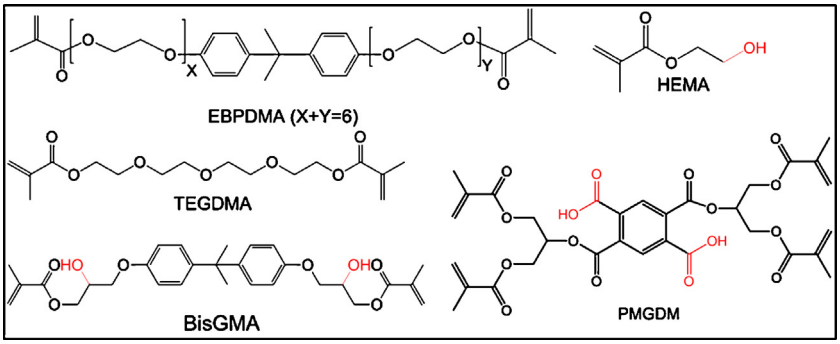

Fig. 1 – Chemical structure of the monomers employed in the study.

AP25 organosols did not form any observable precipitate for months at room temperature.

The compositions of the experimental resins employed in the study are given in Table 1. The experimental formulations activated for light photo-polymerization were stored in the dark before being utilized. The AP25 ethanol organosols were mixed into the activated resins by 10 min agitation at 500 rpm. The ethanol was then removed via air blowing at room temperature for 24 h. Resins with different mass fractions (0 mass %, 0.02 mass %, 0.05 mass %, 0.1 mass %, 0.2 mass %and 0.5 mass %) of AP25 were also prepared.

Disk specimens for degree of vinyl conversion (DC) and water contact angle (WCA) measurements (five disks/experimental group) were prepared in a following manner: a mixture of monomers and AP25 was pipetted into a TEFLON cylinder mold (6 mm in diameter and 1.5 mm thick) placed on top of a piece of Mylar film and a glass slide. Once filled, the top of the mold was covered sequentially with Mylar film and a glass slide, and the assembly was clamped together. The specimens were cured using a Triad 2000 visible light curing unit (Dentsply, York, PA, USA) with a tungsten halogen light bulb (75 W and 120 V, 43 mW/cm^2) for 2 min each from both open sides of the assembly.

2.2. *Polymerization of BMA in the presence of nanoparticles*

The benzyl methylmethacrylate (BMA, Sigma–Aldrich, St. Louis, MO, USA) was photo-polymerized in the presence of 0.1% by mass of P25 or AP25 NPs using 1 wt% of bis(2,4,6-trimethylbenzoyl) phenylphosphine oxide (BPPO, Sigma–Aldrich, St. Louis, MO, USA) as an initiator. The mixture was cured by illuminating with a Blak-Ray 100 W UV lamp (365 nm) at a 20 cm distance (intensity of 10 mW/cm^2) for 3 min, then the polymer was dissolved in toluene and centrifuged to collect precipitates. The dissolving and centrifugation processes were repeated three times, and the final powder were collected, dried and evaluated using Fourier transform infrared (FTIR).

2.3. *Characterization methods*

FTIR spectroscopic measurements were carried out with the Nexus 670 FTIR spectrophotometer (Thermo Scientific, Madison, Wisconsin). NPs were mixed with KBr powder (1.5 mg AP25 and 150 mg KBr) and pressed into pellets. These pellets were examined in transmission mode. Resins and composites were evaluated through an attenuated total reflectance setup. A total of 64 scans were collected from 4000 cm^{-1} to 650 cm^{-1} at 4 cm^{-1} resolution. All measurements were done in triplicate ($n = 3$).

EPR measurements were carried out on a BRUKER BioSpin ElexSys500 spectrometer, using an x-band square cavity (TE011 mode) operating under identical parameter settings: microwave frequency ≈9.38 GHz, field modulation = 100 kHz, and microwave power = 10 mW. Each specimen was placed in a capped quartz EPR tube (0.4 mm thin wall tube, 20 cm long) in the EPR cavity. A 500 W Xe Arc lamp was used as the UV source for in-situ irradiation experiments. All spectra were obtained at 77 K by sweeping the static magnetic field and recording the first derivative of the absorption spectrum. Unexposed specimen and empty EPR tubes were tested, respectively, for reference spectra. A weak pitch standard sample was measured under identical instrumental conditions periodically to correlate the position of EPR signals and double integrals of EPR spectra were analyzed to determine the intensity of peaks. Powder samples were dried before loading into the EPR tubes. The resin and resin composites were in the form of bars (25 × 2 × 2 mm^3). Measurements were repeated twice ($n = 2$).

The UV–vis spectra were collected using a multimode microplate reader (SpectraMax, Model M5, Molecular Devices LLC, CA, USA). The NPs were dispersed in water via ultrasonication (100% amplitude, 130 W Ultrasonic processor, Cole Parmer, USA) for 30 min at a concentration of 0.01 mass %, and transferred to a 96-well plate. Each well contained 0.2 mL samples. The spectra were collected from 200 nm to 1000 nm at 10 nm interval at room temperature. Water was used as a background. Number of repetitive runs/group, $n = 5$.

In 2 mL quartz cuvettes, MB dye-TiO_2 suspensions were prepared to contain 5.5 μM of MB with P25 or AP25 1 mM in ethanol. These solutions were exposed to light irradiation using a Triad 2000 Curing Unit. Irradiation time interval was 20 s for a total exposure of 200 s. Hitachi U2000 Spectrophotometer (Hitachi instrument Inc, San Jose, CA, USA) was used to collect absorbance spectra. The ODs of MB monomer (at 664 nm), dimer (at 606 nm) and trimer (at 570 nm) were measured before and after 200 s irradiation, and the percentage of the OD decrease after light illumination were calculated as the MB degradation in each form.

Please cite this article in press as: Sun J, et al. Tuning photo-catalytic activities of TiO_2 nanoparticles using dimethacrylate resins. Dent Mater (2015), http://dx.doi.org/10.1016/j.dental.2015.11.021

Table 1 – Composition (mass fraction, %) of the experimental resins.

Resin/monomer	Bis-GMA	EBPDMA	PMGDM	TEGDMA	HEMA	CQ	4E
B/T = 3/1	74.25	–	–	24.75	–	0.2	0.8
B/T = 1/1	49.50	–	–	49.50	–	0.2	0.8
B/T = 1/3	24.75	–	–	74.25	–	0.2	0.8
B/H = 1/1	49.50	–	–	–	49.50	0.2	0.8
EBPDMA	–	99.00	–	–	–	0.2	0.8
P/H = 3/1	–	–	74.25	–	24.75	0.2	0.8
P/H = 1/1	–	–	49.50	–	49.50	0.2	0.8
P/H = 1/3	–	–	24.75	–	74.25	0.2	0.8

Dynamic light scattering (DLS) measurements were performed on a Brookhaven instrument (90PLUS/BI-MAS mode, Brookhaven Instruments Cooperation, New York, USA) at 90° angle, 25 °C, in ethanol. A 15 mW solid state laser with a wavelength of 532 nm was used. The hydrodynamic radius (R_h) of particles and its distribution was calculated employing the Brookhaven Instruments-provided software by the method of cumulants using one- or two-exponential fits [24,25]. Measurements were repeated three times ($n = 3$).

2.4. Degree of vinyl conversion (DC)

The DC of resin and composite specimens was determined using near infrared spectroscopy (NIR) [26–28]. NIR spectra were acquired before photo cure and at 24 h post cure. DC was calculated as the percentage change in the integrated peak area of the 6,165 cm^{-1} vinyl on methacrylate absorption band normalized to the 4623 cm^{-1} aromatic C—H absorption band area between the polymer (value after cure) and monomer (values before cure). The standard uncertainty associated with the DC measurement was <1%.

2.5. Water contact angle (WCA) measurement

The WCA measurements were carried out using the sessile drop method with a Kruss G2 system (Hamburg, Germany) at room temperature. The volume of the deionized water droplet was 2 μL, and the images of the sessile droplet were taken immediately after deposition on the substrate. Water contact angle on resins/resin composites were acquired before UV irradiation, 24 h post irradiation and one month after UV irradiation. The films were illuminated with a Blak-Ray 100 W UV lamp (365 nm) at a 20 cm distance (intensity of 10 mW/cm^2) for 20 min. UV irradiation was applied here to maximize the photo-catalytic activities of the TiO_2 nanoparticles in a reasonably short period of time.

2.6. Statistical analysis

One-way analysis of variance (ANOVA) with a 95% confidence interval was used to indicate significant differences between the experimental groups.

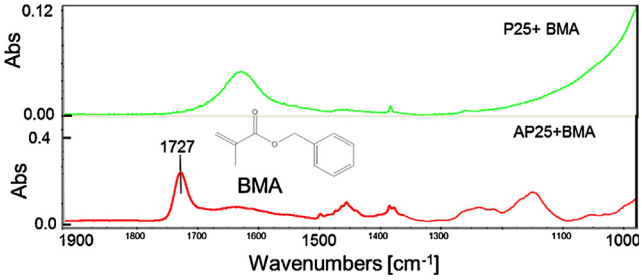

Fig. 2 – FTIR spectra of P25/AP25 after co-polymerized with BMA.

3. Results and discussion

3.1. Functionalization and characterization of TiO_2 nanoparticles

The presence and reactivity of C=C bond on AP25 was confirmed through FTIR and polymerization of BMA in the presence of P25/AP25 NPs. FTIR spectrum of AP25 [9,23] indicated that the acrylic acid was successfully attached onto P25. The —C=C— signal at 1636 cm^{-1} in the FTIR spectrum of AP25 verified the existence of the double bonds on the surface of AP25. In order to better understand the reactivity of the —C=C— bond on AP25 during photo-polymerization, an experiment was designed to evaluate these double bonds on nanoparticles directly and determine their ability for copolymerizing with other monomers. The monomer used in this evaluation was BMA which had only one polymerizable C=C bond. The corresponding polymer, PBMA, was soluble in toluene.

FTIR indicated that the PBMA was attached on AP25 but not on P25. Fig. 2 shows the FTIR spectra of particles after co-polymerization with BMA and isolated by rinsing with toluene and centrifugation. The carbonyl stretch (C=O) of ester on PBMA at 1727 cm^{-1} was only found on particles collected in the PBMA + AP25 mixture. When BMA monomers were polymerized in the presence of P25, the product, PBMA, was dissolved in toluene and separated from P25 particles through centrifugation; no PBMA was attached on P25. On the other hand, PBMA was found on functionalized nanoparticles of AP25. BMA copolymerized with C=C on AP25 and formed nanocomposites, which could be dispersed in toluene and collected as particles through centrifugation.

This experiment confirmed that the C=C on AP25 copolymerized with resins during photo-polymerization, thus likely

Please cite this article in press as: Sun J, et al. Tuning photo-catalytic activities of TiO_2 nanoparticles using dimethacrylate resins. Dent Mater (2015), http://dx.doi.org/10.1016/j.dental.2015.11.021

creating rigid, more cross-linked polymer network. The covalent bonds between the NPs and the resin via short-chain unsaturated groups are a powerful tool for enhanced mechanical performance of dental resins [9,29]. Previous studies showed that the mechanical performance of dimethacrylate resins were dramatically enhancement by adding a very small amount (<0.1 mass %) of NPs functionalized with C=C bonds [9].

The PCAs of TiO_2 NPs are generally evaluated by: (1) the NPs' capability to absorb low energy light, especially visible light; and (2) the NPs' ability to generate and maintain radicals [2]. In this work, we used EPR, UV–vis and degradation of methylene blue to compare the PCAs of the unfunctionalized P25 and functionalized AP25 TiO_2 NPs.

Fig. 3A and B shows the EPR spectra of P25 and AP25, respectively. In both figures, the red line indicates the spectra of nanoparticles without UV irradiation and the blue lines are the spectra of nanoparticles after 1 h UV irradiation. Both P25 and AP25 contained more radicals after UV irradiation, but their EPR spectra and the radical evolution over time of UV irradiation are different. Without UV irradiation, the EPR signal of P25 is low, below an intensity of 2.5. After UV irradiation, the EPR signal increases, and more electrons than holes are detected. Comparatively, before UV irradiation, AP25 starts with a stronger EPR signal, at an approximate intensity of 10. After UV irradiation, the EPR signal also increased; but more holes instead of electrons are detected. The EPR results indicate that P25 and AP25 are chemically different. The kinetics of radical production and radical life time are different as well.

Fig. 3C shows radical evolution over irradiation time and the lifetime of these radicals. In this figure, square symbols and circle symbols stand for the amount of radicals (electrons and holes) on P25 and AP25 as a function of time, respectively; solid symbols show the amount of radicals as a function of time under UV irradiation, and open symbols indicate the amount of radicals over time after irradiation. Both of the nanoparticles show exponential increase of radicals under UV irradiation. The amount of radicals grows fast initially and then plateau. P25 nanoparticles reach plateau within 30 min, while AP25 nanoparticles reach the maximum levels after 1 h of UV irradiation. In addition, the maximum amount of radicals on AP25 nanoparticles is approximately 2.5 times the amount generated on P25. Moreover, after UV irradiation has stopped, the radicals on AP25 nanoparticles are stable for more than 30 min, while the radicals on P25 disappear instantly.

The functionalization of TiO_2 NPs enhanced the capability of nanoparticles to produce radicals, and the life time of radicals on nanoparticles after functionalization was greatly improved. In the case of the unfunctionalized TiO_2 NPs, electrons and holes combined with each other resulting in the reduced number of free radicals. However, in the case of the functionalized TiO_2 NPs (AP 25), the recombination of electrons and holes appears to be prevented by the attached functional groups thus yielding NPs with the enhanced radical capacity and life time.

DLS results indicated that both particles formed small agglomerates in ethanol and the hydrodynamic radius of their agglomerate were the same, 77 ± 2 nm, with narrow sized distribution. In addition, TEM results showed that the

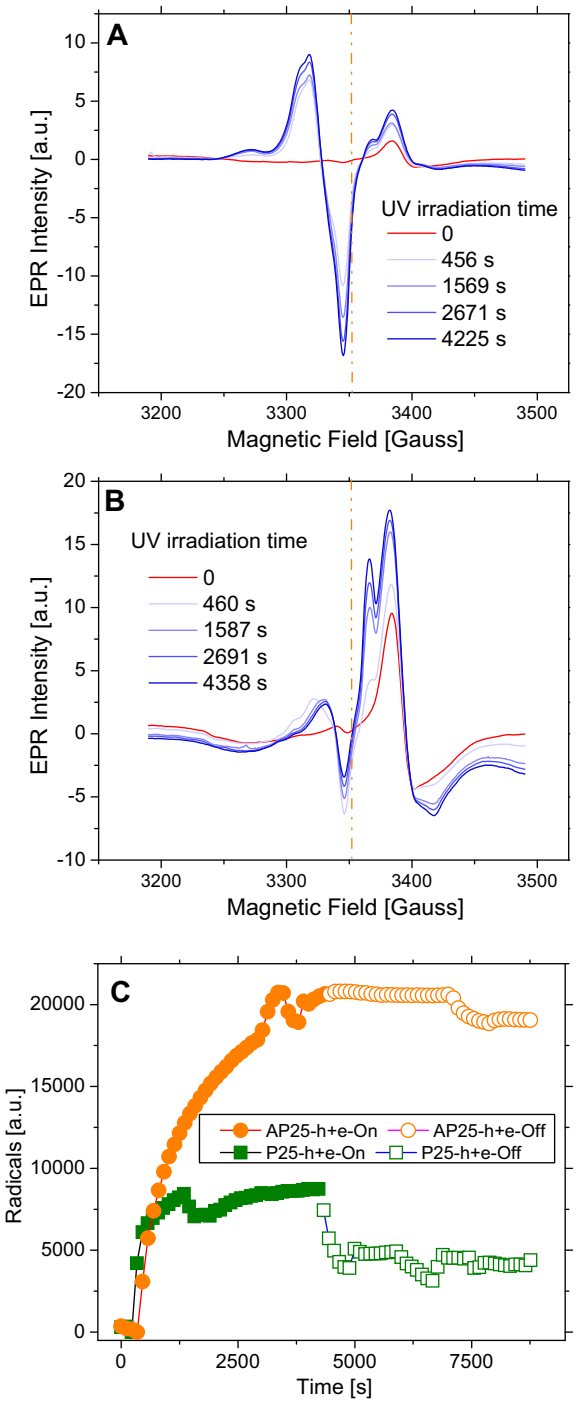

Fig. 3 – (A) EPR spectra of P25 NPs before and after UV irradiation; (B) EPR spectra of AP25 NPs before and after UV irradiation; (C) radicals (electrons and holes) forming on P25 NPs (green) and AP25 NPs (orange) as a function of time under UV irradiation. Open symbols indicate the change of radicals over time after cessation of UV irradiation. (For interpretation of the references to color in this figure legend, the reader is referred to the web version of this article.)

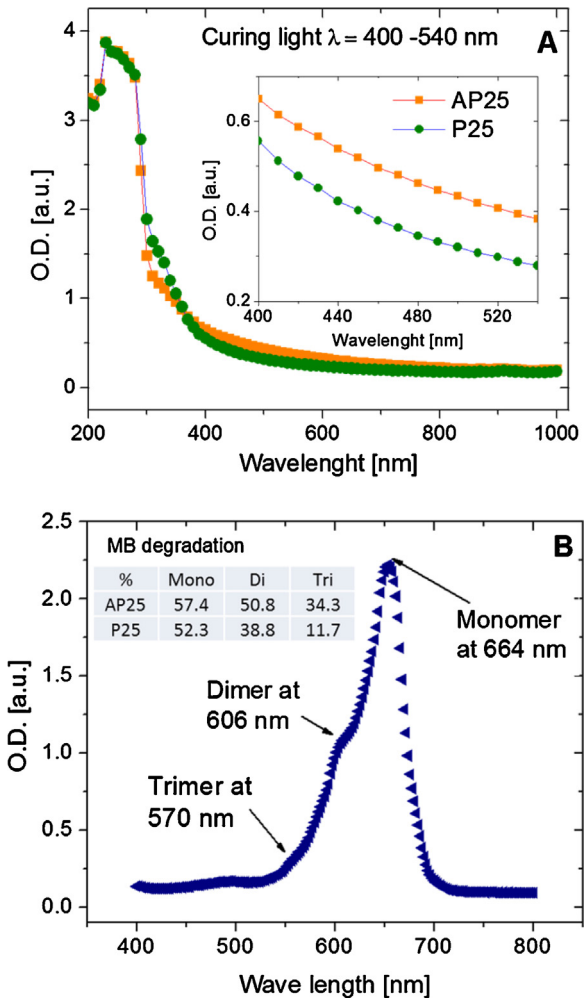

Fig. 4 – (A) UV–vis absorbance spectrum of P25 (green) and AP25 (orange) in ethanol. Inset: the absorbance of the same NPs in the visible light region. (B) UV–vis spectra of MB in ethanol. Inlet (Table): the percentage of the MBs degraded after 200 s light irradiation. (For interpretation of the references to color in this figure legend, the reader is referred to the web version of this article.)

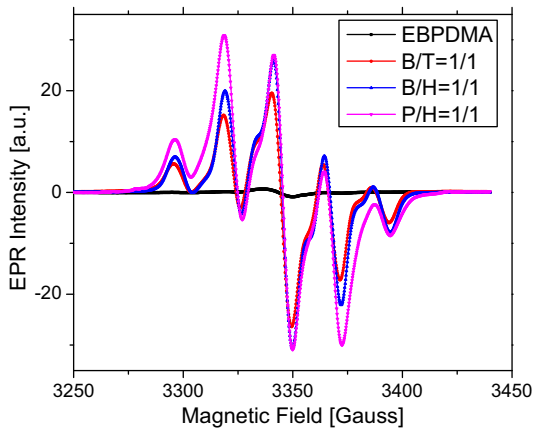

Fig. 5 – EPR spectra of the selected experimental resins in set one under strong magnetic field.

functionalization of P25 did not alter the average diameter of individual nanoparticle [9].

The UV–vis absorbance spectra (Fig. 4A) indicates slight absorbance increase in the visible light region from 400 nm to 540 nm, which is the active wavelength range for light curing unit, Triad 2000. The PCAs of nanoparticles were further evaluated by the decomposition of methylene blue (MB) under light irradiation in Triad 2000 unit which is widely used in dental research for curing dental resins and dental resin composites. MB has at least three forms in solution. As illustrated in Fig. 4B, monomer MB (absorbance peak at 664 nm) is the majority, then dimer (absorbance peak at 606 nm), and then trimer (absorbance peak at 570 nm). Other forms of MB may also exist but in very low concentrations, so they were not evaluated. The inset table in Fig. 4B lists the percentage of the MBs degraded after 200 s light irradiation. Clearly, AP25 decomposed more MBs than P25. Above all, AP25 had better PCAs comparing with P25, and the presence of functional groups on the surface enhances the bonding of nanoparticles to the resin network. This study is focusing on the functionalized nanoparticles, AP25, and its PCAs in different resins.

3.2. *Grouping resins based on chemical structure and viscosity of monomers*

Superoxide and hydroxyl free radicals are both strong oxidants. Oppositely, hydroxyl and carboxyl groups are effective functional groups in many antioxidants. Therefore, the content of hydroxyl and carboxylic groups of the monomers was one of the major criteria for resin selection. Viscosity and hydrophilicity of resin monomers were also considered.

The eight resin compositions (Table 1) are divided into two sets based on the chemical structure and viscosity of monomers. One set includes EBPDMA, B/T = 1/1, B/H = 1/1, and H/P = 1/1. In this set, the variation of chemical structures (the number of hydroxyl and carboxyl groups) lead the trend in radical intensity under strong magnetic fields, LogP, and hydrophilicity of these resins (Table 2). The other set contains six resin compositions of B/T and P/H systems. By varying the mass ratio (3/1, 1/1 and 1/3) of base resin (Bis-GMA or PMGDM) and the corresponding diluent resin (TEGDMA or HEMA), three distinguishable viscosities are created in two chemical systems. P/H systems contain more hydroxyl and carboxyl groups than B/T systems.

Table 2 shows the trends in chemical structure change (the number of hydroxyl groups and carboxyl groups), radical concentration, partition-coefficient (LogP), and hydrophilicity [30,31] of the selected experimental resins in set one. The number of hydroxyl groups and carboxyl groups was calculated (monomer structures are indicated in Fig. 1), and the LogP of resin monomers was predicted using ChemBioDraw (verision 14, ParkinElmer Informatic, USA). The radical level in these resins, measured by EPR, revealed that the trend was identical to the change in number of hydroxyl and carboxyl groups (Fig. 5). In addition, these four resins also shared the same trend in hydrophilicity (experimentally evaluated through WCA measurements) as that in the number of hydroxyl and carboxyl groups.

Please cite this article in press as: Sun J, et al. Tuning photo-catalytic activities of TiO_2 nanoparticles using dimethacrylate resins. Dent Mater (2015), http://dx.doi.org/10.1016/j.dental.2015.11.021

Table 2 – Trends in the number of hydroxyl and carboxyl groups, radical intensity under strong magnetic fields, LogP, and hydrophilicity of the resins in set one.

Resins	Number of OH groups	Radicals by EPR	logP	Hydrophilicity
EBPDMA	Zero	Less	High	
B/T = 1/1	↓	↓	↑	↓
B/H = 1/1				
P/H = 1/1	High	More	Low	More hydrophilic

Table 3 – Viscosity, LogP and number of OH/COOH groups of monomers.

Monomer	Viscosity (cP)*	LogP	OH/COOH groups/molecular
PMGDM	Solid	3.73	2 COOH groups
Bis-GMA	700,000	5.05	2 OH groups
EBPDMA	450	6.17	0
B/T = 1/1	225	–	1 OH group
TEGDMA	12	1.27	0
HEMA	5.9	0.47	1 OH group

An important property that could affect monomer conversion in photo-polymerization is the viscosity of the resin monomers. To emphasize the impact of viscosity on DC, two categories of resin systems with distinguished chemical differences and containing three viscosity variations were compared: B/T and P/H resin systems. The mixtures in the B/T systems were relatively hydrophobic with fewer hydroxyl or carboxyl groups. The P/H systems were generally more hydrophilic with more hydroxyl and carboxyl groups. In each catagory, there was a base monomer, Bis-GMA or PMGDM, which was more viscous than the other monomer, the diluent monomer, TEGDMA or HEMA. By changing the mass ratios of the base and diluent monomers, three distinguishable viscosities were attained within B/T or P/H systems. The viscosity of the resins increased with the content of Bis-GMA or PMGDM in the following order: B/T or P/H = 1/3 < B/T or PH = 1/1 < B/T or P/H = 3/1 (Table 3).

3.3. *The effects of chemical structure and viscosity on DC improvement*

The effect of chemical structure of constituent monomers on DC improvement was evaluated in resins indicated in Table 2 (EBPADMA, B/T, B/H and P/H resins). DC of the composites generally increased with the increasing levels of AP25 incorporated into resins (Fig. 6A), furthermore, the extent of the increase varied from resin to resin. EBPDMA showed the highest increase (22.9%) in DC with the addition of A25. Lesser effect on DC was seen in B/T resins (increase in DC of up to 14.9%) and in P/H or B/H resins (less than 10% increase in DC – both resins). Consequently, a following order of DC improvement was obtained due to the addition of TiO_2 NPs to the resin compositions of comparable viscosities (200–500 cP): EBPDMA > B/T > (P/H ≥ B/H), which is in good agreement with the trend of chemical structure and properties listed in Table 2.

Viscosity effects on DC improvement attained in B/T and P/H resin systems with and without NPs are shown in Fig. 6B. Chosen 3/1, 1/1 and 1/3 mass ratios of the base (BisGMA or PMGDM) vs. diluent monomer (TEGMDA or HEMA) yielded three distinct levels of resin viscosity, categorized as high viscosity (more than 1000 cP), medium viscosity (200–500 cP) and low viscosity (below 100 cP). Without the NPs, in both B/T and P/H series, DC increased from the high viscosity resins

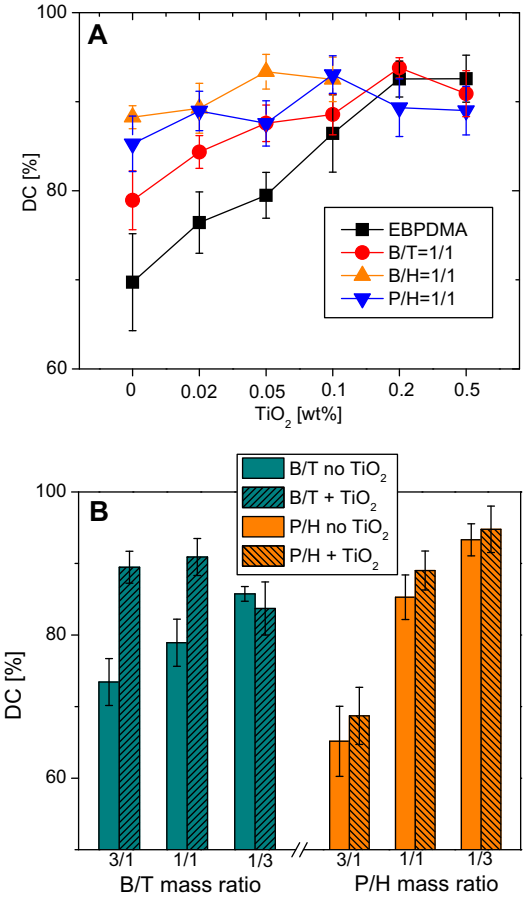

Fig. 6 – (A) The DC of resins increased as a function of mass % of AP25; (B) It shows DCs of two groups of B/T and P/H monomers with/without 0.5 mass % AP25 NPs.

to low viscosity ones. Bis-GMA- and PMGDM-rich mixtures exhibited the lowest DC while diluent monomer (TEGDMA or HEMA)-rich resins exhibited the highest DC. The above results agree well with the findings in free radical polymerization of methacrylate monomers, where in the later stage of polymerization, the chain termination reaction and chain propagation reaction become diffusion controlled; as a result, less mobile

Please cite this article in press as: Sun J, et al. Tuning photo-catalytic activities of TiO_2 nanoparticles using dimethacrylate resins. Dent Mater (2015), http://dx.doi.org/10.1016/j.dental.2015.11.021

monomers (higher viscosity monomers) have a lower double bond conversion [32–34].

One would expect that any observable improvement in DC resulting from the introduction of TiO_2 NPs into the resins at levels employed in this study (up to 0.5 mass %), would be due to the chemical interactions with the resin monomers rather than viscosity alterations. In the P/H system, no statistically significant difference ($p < 0.05$) in DC was observed when comparing pure resins and composites with 0.5 mass % NPs (Fig. 6B). While in the B/T system, adding NPs to the resins had multifaceted effects. For B/T = 3/1 and B/T = 1/1 monomers, addition of AP25 resulted in a significant improvement in DC (maximum DC values were comparable in these two systems), but the B/T = 1/3 monomer showed no improvement in DC following the addition of 0.5 mass % AP25. This may be due to the intrinsically higher DC of B/T = 1/3 (85.7 ± 1%) leaving a small amount of available monomers for further DC improvement. The DC of B/T = 3/1 and B/T = 1/1 without AP25 addition was lower, 73.4 ± 3.3% and 78.9 ± 3.3%, respectively. In both compositions, the unreacted monomers react with added AP25 NPs and yield 11–16% DC increase in the ensuing composites.

The TiO_2 NPs further enhanced the DC of dental resins in addition to the double bond conversion initiated by CQ/4E system. The effects were more pronounced in monomers that are more hydrophobic/containing less hydroxyl groups or/and carboxyl groups. Unlike the CQ/4E initiator system, the viscosity of resin monomers played minimum or no roles in the DC improvement by adding TiO_2 NPs. Beneficial effects of the increased DC of TiO_2-containing nano-composites include reduced amount of unreacted monomers, which may leach into bio-environment, and potentially more rigid and harder composites [9]. However, resins with improved DC are not necessary superior in mechanical performance. Depending on the application, the overall performance of the nanocomposites need to be balanced with other factors including but not limited to: wettability, dispersion of NPs, interaction of NPs with resin monomers, and polymerization shrinkage.

3.4. *Water contact angle measurements and wettability of nanocomposites*

Water contact angle (WCA) measurement is a simplified way to directly compare the hydrophilicity (surface wettability to water) of material surfaces. Lower WCA indicates relatively more hydrophilic surface; superhydrophilic surfaces have WCA below five degree [35]. Biologic and clinical studies indicated that surface hydrophilicity of materials is one of the key factors to improve the performance of tissue engineering materials [36]. Hydrophilic surfaces tend to enhance the early stages of cell adhesion, proliferation, differentiation and bone mineralization compared to hydrophobic surfaces [37].

The WCAs of the resins and their AP25-containing composites before and after UV irradiation are compared in Fig. 7A and B. Before UV irradiation, the WCAs of both pure resins and their AP25 composites followed the order predicted by LogP (Table 2): EBPDMA > B/T = 1/1 > P/H = 1/1. Adding nanoparticles to the resins increased the hydrophilicity, and the composites (resin with 0.5 mass % nanoparticles) had smaller WCAs angles than pure resins. The WCAs of P/H and EBPDMA resins were significantly greater than the WCAs of their corresponding AP25 composites. However, the WCAs of B/T resins and their AP25 composites were statistically indistinguishable according to one-way ANOVA, even the mean value of the WCAs of the B/T resin was bigger.

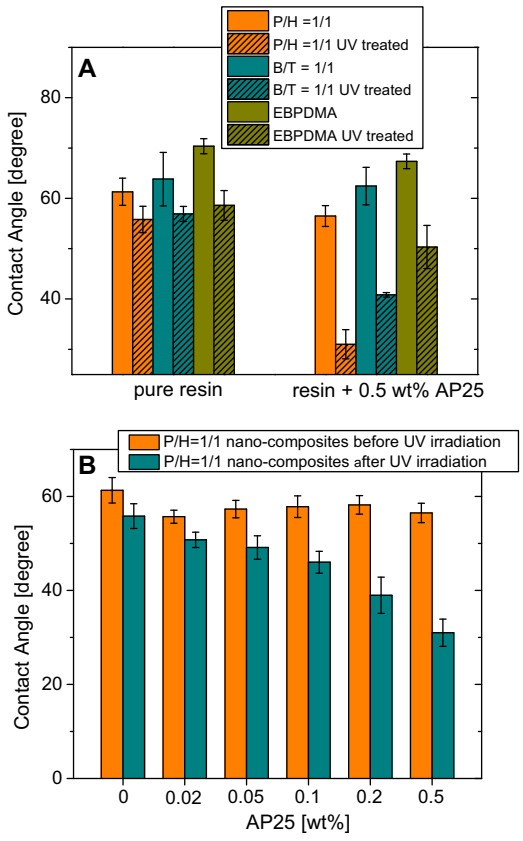

Fig. 7 – (A) The WCAs of the resins (without AP25) and their corresponding composites containing 0.5 mass % AP25 NPs – before and after UV irradiation. (B) The WCAs of the P/H = 1/1 resin and the composites with different AP25 NPs content – before and after UV irradiation.

After UV irradiation, the WCAs of all resins and their AP25 composites decreased to different degrees. The WCAs of EBPDMA, B/T and P/H resins were the same suggesting that the relatively more hydrophobic EBPDMA resin changed more than the relatively more hydrophilic B/T and/or P/H resins upon UV irradiation. On the other hand, UV irradiation had dramatically different impacts on AP25 composites (Fig. 7A). The P/H = 1/1 composite had the largest WCA drop, followed by B/T = 1/1 composite and EBPDMA composite; the order coincides with a decrease in resin's hydrophilicity. The most hydrophilic composite showed the largest improvement in surface hydrophilicity by adding AP25 NPs. In addition, the WCAs also changed with concentration of added AP25 (Fig. 7B). In P/H = 1/1 composites, more AP25 NPs resulted in greater hydrophilicity upon UV irradiation. These findings suggest that the radicals generated through AP25 NPs could modify surface hydrophilicity more than UV irradiation alone. More significantly, the extent of this modification could be controlled by varying the amount of NPs and the composition of resins. The hydrophilicity change induced by the UV irradiation preserved in the resins and composites. After UV

Please cite this article in press as: Sun J, et al. Tuning photo-catalytic activities of TiO_2 nanoparticles using dimethacrylate resins. Dent Mater (2015), http://dx.doi.org/10.1016/j.dental.2015.11.021

irradiation, the specimens were stored in dark for one month. No statistically significant difference ($p > 0.05$) in WCAs was observed when comparing the WCAs of the specimens measured immediately after and one month after UV irradiation.

UV irradiation may cause chemical changes in both resins and composites. FTIR was not sensitive enough to identify the chemical changes on pure resins. EPR spectra indicate neither chemical change in EBPDMA resin nor chemical changes in EBPDMA composites after UV irradiation. However, FTIR shows that the absorbance at 1561 cm^{-1}, corresponding to the O=C—O functional group, in P/H composites disappeared after UV irradiation. The absence of this particular peak in FTIR spectrum is most likely due to carboxylate/TiO_2 interaction in P/H–AP25 composites. In addition, a red-shift of —OH groups above 3400 cm^{-1} was observed, possibly due to hydrogen bonding [38]. The WCA results and FTIR findings combined indicate that the radicals produced by NPs generate permanent chemical changes in the composites. These changes may be triggered by decomposition of carboxyl groups and forming of hydrogen bonds.

4. Conclusions

Functionalizing TiO_2 NPs with short-chain unsaturated carboxylic acid enhanced radical loading on NPs by 2.5 times under light irradiation, and life time of radicals was increased over 10 times. The double bonds on the functionalized TiO_2 NPs (AP25) were active in copolymerizing with other monomers through free radical photopolymerization. The addition of AP25 enhanced DC in an order: EBPDMA > B/T > (P/H ≥ B/H), which was in a reverse trend of chemical structure variation, i.e., increasing number of hydroxyl and carboxyl groups in monomers, and hydrophilicity. As co-initiator to CQ/amine initiator systems, TiO_2 NPs were more effective in promoting conversion of monomers into polymers in the resin systems with less hydroxyl and carboxyl groups. Viscosity plays minimal or no role in DC improvement through TiO_2 NPs. This finding differs from the viscosity effects seen in the pristine CQ/amine resin systems, in which high viscosity resin monomers yielded low DCs. When using TiO_2 NPs to modify wettability of resins under UV irradiation, the AP25 was more active in resin systems with more hydroxyl and carboxyl groups. The hydrophilicity of P/H = 1/1 increases as a function of mass fraction of TiO_2 NPs thus providing a potential to design materials with controllable wettability, desirable in many applications, including implants and scaffolds for tissue engineering.

Above all, TiO_2 NPs are useful additives in achieving dramatic performance improvement at very small fraction in the resins. Furthermore, their applications can be tuned through the functional groups including hydroxyl and carboxyl groups. The findings of this study open new possibilities to balance material performance without significantly changing the composition of the materials.

Acknowledgements

This work is partially funded by the National Institute of Dental and Craniofacial Research (U01DE023752). Financial support was also provided through ADA Foundation. The authors would like to thank Mr. Anthony Giuseppetti and Dr. Joseph Antonucci for their technical recommendations. We also would like to thank Center for Nanoscale Science and Technology (CNST) at NIST for their technical support.

REFERENCES

[1] Carp O, Huisman CL, Reller A. Photoinduced reactivity of titanium dioxide. Prog Solid State Chem 2004;32:33–177.
[2] Chen XB, Liu L, Yu PY, Mao SS. Increasing solar absorption for photocatalysis with black hydrogenated titanium dioxide nanocrystals. Science 2011;331:746–50.
[3] Fujishima A, Honda K. Electrochemical photolysis of water at a semiconductor electrode. Nature 1972;238:37–8.
[4] Oregan B, Gratzel M. A low-cost, high-efficiency solar-cell based on dye-sensitized coloidal TiO_2 films. Nature 1991;353:737–40.
[5] Qiu XQ, Miyauchi M, Sunada K, Minoshima M, Liu M, Lu Y, et al. Hybrid CuxO/TiO_2 nanocomposites as risk-reduction materials in indoor environments. ACS Nano 2012;6:1609–18.
[6] Karimi L, Yazdanshenas ME, Khajavi R, Rashidi A, Mirjalili M. Using graphene/TiO_2 nanocomposite as a new route for preparation of electroconductive, self-cleaning, antibacterial and antifungal cotton fabric without toxicity. Cellulose 2014;21:3813–27.
[7] Campoccia D, Montanaro L, Arciola CR. A review of the biomaterials technologies for infection-resistant surfaces. Biomaterials 2013;34:8533–54.
[8] Xiao J, Chen WQ, Wang FYK, Du JZ. Polymer/TiO_2 hybrid nanoparticles with highly effective UV-screening but eliminated photocatalytic activity. Macromolecules 2013;46:375–83.
[9] Sun JR, Forster AM, Johnson PM, Eidelman N, Quinn G, Schumacher G, et al. Improving performance of dental resins by adding titanium dioxide nanoparticles. Dent Mater 2011;27:972–82.
[10] Yoshida K, Taira Y, Atsuta M. Properties of opaque resin composite containing coated and silanized titanium dioxide. J Dent Res 2001;80:864–8.
[11] Yu B, Ahn JS, Lim JI, Lee YK. Influence of TiO_2 nanoparticles on the optical properties of resin composites. Dent Mater 2009;25:1142–7.
[12] Fu GF, Vary PS, Lin CT. Anatase TiO_2 nanocomposites for antimicrobial coatings. J Phys Chem B 2005;109:8889–98.
[13] Feng XJ, Zhai J, Jiang L. The fabrication and switchable superhydrophobicity of TiO_2 nanorod films. Angew Chem-Int Ed 2005;44:5115–8.
[14] Mills A, LeHunte S. An overview of semiconductor photocatalysis. J Photochem Photobiol A: Chem 1997;108:1–35.
[15] Mills A, Lee SK, Lepre A. Photodecomposition of ozone sensitised by a film of titanium dioxide on glass. J Photochem Photobiol A: Chem 2003;155:199–205.
[16] Darrah PA, Hondalus MK, Chen QP, Ischiropoulos H, Mosser DM. Cooperation between reactive oxygen and nitrogen intermediates in killing of *Rhodococcus equi* by activated macrophages. Infect Immun 2000;68:3587–93.
[17] Pacher P, Beckman JS, Liaudet L. Nitric oxide and peroxynitrite in health and disease. Physiol Rev 2007;87:315–424.
[18] Fang YZ, Yang S, Wu GY. Free radicals, antioxidants, and nutrition. Nutrition 2002;18:872–9.
[19] Halliwell B. Oxidative stress and neurodegeneration: where are we now. J Neurochem 2006;97:1634–58.

Please cite this article in press as: Sun J, et al. Tuning photo-catalytic activities of TiO_2 nanoparticles using dimethacrylate resins. Dent Mater (2015), http://dx.doi.org/10.1016/j.dental.2015.11.021

[20] Britton G. Structure and properties of carotenoids in relation to function. FASEB J 1995;9:1551–8.
[21] Heim KE, Tagliaferro AR, Bobilya DJ. Flavonoid antioxidants: chemistry, metabolism and structure–activity relationships. J Nutr Biochem 2002;13:572–84.
[22] RiceEvans CA, Miller NJ, Paganga G. Structure–antioxidant activity relationships of flavonoids and phenolic acids. Free Radic Biol Med 1996;20:933–56.
[23] Vo DQ, Kim EJ, Kim S. Surface modification of hydrophobic nanocrystals using short-chain carboxylic acids. J Colloid Interface Sci 2009;337:75–80.
[24] Koppel DE. Analysis of macromolecular polydispersity in intensity correlation spectroscopy – method of cumulants. J Chem Phys 1972;57:4814–20.
[25] Riseman J, Kirkwood JG. The intrinsic viscosity, translational and rotatory diffusion constants of rod-like macromoleculres in solution. J Chem Phys 1950;18:512–6.
[26] Stansbury JW, Dickens SH. Determination of double bond conversion in dental resins by near infrared spectroscopy. Dent Mater 2001;17:71–9.
[27] Eidelman N, Raghavan D, Forster AM, Amis EJ, Karim A. Combinatorial approach to characterizing epoxy curing. Macromol Rapid Commun 2004;25:259–63.
[28] Antonucci JM, Fowler BO, Weir MD, Skrtic D, Stansbury JW. Effect of ethyl-alpha-hydroxymethylacrylate on selected properties of copolymers and ACP resin composites. J Mater Sci: Mater Med 2008;19:3263–71.
[29] Wilson KS, Allen AJ, Washburn NR, Antonucci JM. Interphase effects in dental nanocomposites investigated by small-angle neutron scattering. J Biomed Mater Res A 2007;81A:113–23.
[30] Nishitani Y, Yoshiyama M, Donnelly AM, Agee KA, Sword J, Tay FR, et al. Effects of resin hydrophilicity on dentin bond strength. J Dent Res 2006;85:1016–21.
[31] Yiu CKY, King NM, Pashley DH, Suh BI, Carvalho RM, Carrilho MRO, et al. Effect of resin hydrophilicity and water storage on resin strength. Biomaterials 2004;25:5789–96.
[32] Khatri CA, Stansbury JW, Schultheisz CR, Antonucci JM. Synthesis, characterization and evaluation of urethane derivatives of Bis-GMA. Dent Mater 2003;19:584–8.
[33] Anseth KS, Wang CM, Bowman CN. Reaction behavior and kinetic constants for photopolymerizations of multi(meth)acrylate monomers. Polymer 1994;35:3243–50.
[34] Brooks BW. Viscosity effects in the free-radical polymerization of methyl methacrylate. Proc R Soc Lond A: Math Phys Sci 1977;357:183–92.
[35] Drelich J, Chibowski E, Meng DD, Terpilowski K. Hydrophilic and superhydrophilic surfaces and materials. Soft Matter 2011;7:9804–28.
[36] Gittens RA, Scheideler L, Rupp F, Hyzy SL, Geis-Gerstorfer J, Schwartz Z, et al. A review on the wettability of dental implant surfaces II: biological and clinical aspects. Acta Biomater 2014;10:2907–18.
[37] Bornstein MM, Valderrama P, Jones AA, Wilson TG, Seibl R, Cochran DL. Bone apposition around two different sandblasted and acid-etched titanium implant surfaces: a histomorphometric study in canine mandibles. Clin Oral Implant Res 2008;19:233–41.
[38] Kuo SW, Chang FC. Studies of miscibility behavior and hydrogen bonding in blends of poly(vinylphenol) and poly(vinylpyrrolidone). Macromolecules 2001;34:5224–8.

Please cite this article in press as: Sun J, et al. Tuning photo-catalytic activities of TiO_2 nanoparticles using dimethacrylate resins. Dent Mater (2015), http://dx.doi.org/10.1016/j.dental.2015.11.021